Journal of Computer Science and Cybernetics, V.35, N.2 (2019), 185–196
DOI 10.15625/1813-9663/35/2/13233

TRACKING CONTROL FOR ELECTRO-OPTICAL SYSTEM IN VIBRATION ENVIROMENT BASED ON SELF-TUNING FUZZY SLIDING MODE CONTROL

DUYEN-HA THI KIM[1], TIEN-NGO MANH[2,*], CHIEN-NGUYEN NHU[2], VIET-DO HOANG[2], HUONG-NGUYEN THI THU[3], KIEN-PHUNG CHI[4]

[1]*Ha Noi University of Industry*
[2]*Institute of Physic, Vietnam Academy of Science and Technology*
[3]*Military Technical Academy*
[4]*Control, Automation in Production and Improvement of Technology Institute*
[*]*ha.duyen@haui.edu.vn*

Abstract. The paper presents a new method for tracking control of EOTS (Electro-Optical Tracking System) operating in mobile environment such as ship, air plane, tank and so on. This makes the base body of the EOTS has angular motion. The control alogorithm used in this paper is adaptive fuzzy sliding mode. The overall control is built and simulated in Matlab and compared with a sliding mode controller and a conventional PID controller. The simulation result illustrated the effectiveness of the proposed controller.

Keywords. Electro-Optical Tracking System; Sliding- Mode Control; Backstepping; Fuzzy; Fuzzy Sliding Mode Control.

Symbols:

Symbol	Unit	Definition
${}^{A}J, {}^{B}J$		The inertia matrices of the pitch and yaw gimbal
T_{Dp}, T_{Dy}	N.m	The torque disturbance of the pitch and yaw gimbal
T_{Dy1}, T_{Dy2}	N.m	The torque disturbance affected the pitch channels rotation cause of the angular motion of the base body and the pitch channels motion (cross-coupling)
T_{Dp1}, T_{Dp2}	N.m	The torque disturbance affected the yaw channels rotation cause of the angular motion of the base body and the yaw channels motion (cross-coupling)
J_{eq}		The instantaneous moment of inertia about k-axis
$\tau_e, \tau_e^{'}$	kg/m2	Moment of motor (up, down)
$\overline{H}$	Kg.m2/s	The angular momentum
$\theta, , \alpha$	Rad	The rotating angles of yaw channel about k-axis and pitch channel about e-axis respectively
$\omega_{Ae},\ \omega_{Bk}$	Rad/s	The body angular velocities of frame A in relation to inertial space r, d, e axes respectively
$\omega_{Pi},\ \omega_{Pj},\ \omega_{Pk}$	Rad/s	The body angular velocities of frame P in relation to inertial space about i,j,k axes respectively

Abbreviations:

EOTS	Electro Optical Tracking System
LOS	Line Of Sight
ISP	Inertial Stabilization Platform
FSMC	Fuzzy Sliding Mode Control
SMC	Backstepping Sliding Mode Control

1. SYSTEM OVERVIEW

The Electro-Optical Tracking System attempts to align its detector axis combined of the pitch and yaw gimbal with a LOS joining the tracker and the target. The tracker contains two loops: outer track loop, and inner stabilization loop as shown in Figure 1 and the method controls are suggested [1, 2, 3, 4, 5, 6, 7, 8, 9, 10, 11, 12, 13, 14, 15, 16, 17, 18].

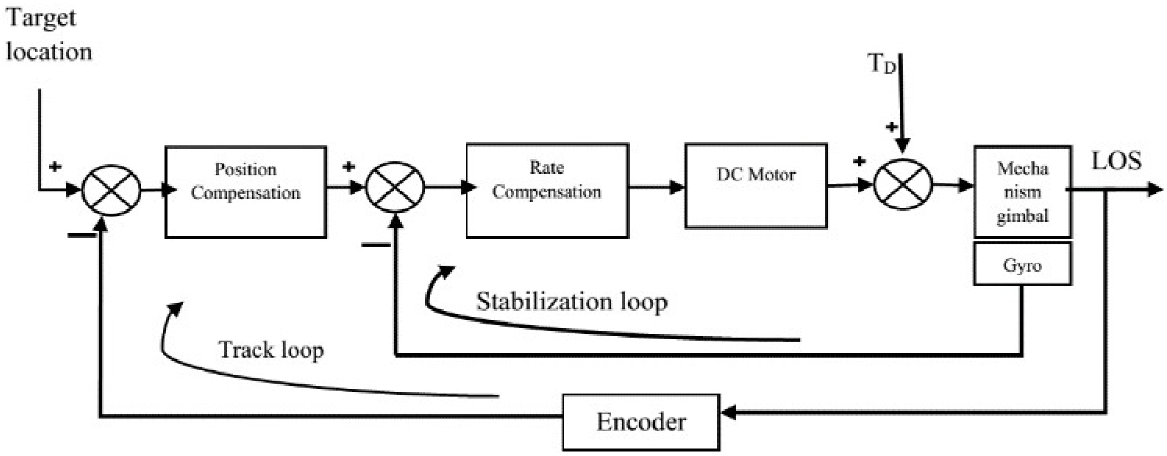

Figure 1. The functional block diagram of stabilization/tracking system for one axis gimbal

The important requirement of the EOTSs is that the optical sensor axis must be accurately pointed to a fixed or moving target even if operating in vibration environment such as ship, air plane, tank [7, 8, 9, 12, 14]. Therefore, the sensors line of sight (LOS) must be strictly controlled [9, 10, 12, 14, 16]. To maintaining sensor orientation toward a target is a serious challenge. An inertial stabilization platform (ISP) is an appropriate way that can solve this challenge [11]. Besides the mathematic model of the system obtained and cross coupling also gave in this section. The term cross coupling which describes the impact of the pitch gimbal to the yaw gimbal and inversely, is based on the relations of the torques affected on them. The cross coupling expresses the properties of the system dynamics. As a result, that is also defined as the effect on one axis by the rotation of another. A two-axis rate gyro is usually placed on the pitch gimbal, measuring the rotational rates in the two directions of interest. These gyro signals are utilized as feedback to torque motors acting on the gimbal.

To maintaining, the sensors LOS is is not simple. The disturbances affecting the operating of EOTS are the disturbance torque because of angular motion of the base body (when EOTS works in vibration environment), cross-coupling effect and so on. Some of the recent papers that research on this academic background can be found. The papers [2, 4] used the conventional PID controller to solve the above challenge. The paper [17] proposed a sliding mode algorithm. Beside, some modern control algorithms such as fuzzy control [3], robust control [13] is applied. The general target of all the above research has just solved the stability of the stabilization loop or the control input is the angular velocity. The track loop or the input is the angular is not mentioned. The paper [15] proposed a self-tuning PID controller for the track loop. Event though, it eliminated the effect of angular motion of the base body when working under vibration condition. A backstepping sliding mode controller designed for the track loop is proposed in the paper [1]. However, the response of the system with this controller is slower than the conventional PID controller and it did not mention the dynamic unbalance effect on the yaw channel.

This paper proposes using the adaptive backstepping sliding mode controller based on fuzzy logic when working under vibration environment and mentioning the effect of dynamic unbalance on the pitch and yaw channel. This controller can guarantee stabilization, the performance of tracking loop and solve the weakness of the PID controller and the backstepping sliding mode controller (has the fast response and good quality control).

The paper is composed of five sections. After this introduction, in the second section, the equation of the gimbal motion is presented. The third section presents the steps to design the proposed controller. The simulation results present in the fourth section and the last section contains the concluding remarks.

2. EQUATIONS OF GIMBAL MOTION

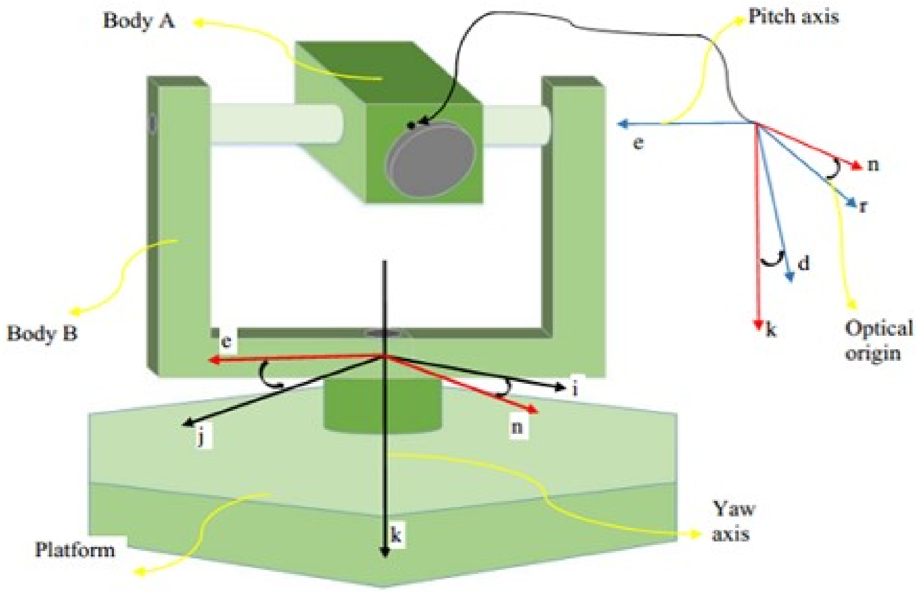

Figure 2. The two-axes gimbal system

Two axes and three reference frames of the two-axis gimbal system are assigned in Figure 2. Frame P fixed to the body with axes (i, j, k), frame B fixed to the yaw channel with axes (n, e, k), and frame A fixed to the pitch channel with axes (d, r, e). The r-axis coincides with the original optical sensor axis. The center of rotation is at the frame origin.

The rotation matrix or the transformation matrix from the frame P to frame B and the transformation matrix from the frame B to frame A

$$ {}_{P}^{B}B = \begin{bmatrix} \cos\alpha & \sin\alpha & 0 \\ -\sin\alpha & \cos\alpha & 0 \\ 0 & 0 & 1 \end{bmatrix}, \ {}_{B}^{A}T = \begin{bmatrix} \cos\theta & 0 & -\sin\theta \\ 0 & 1 & 0 \\ \sin\theta & 0 & \cos\theta \end{bmatrix}, \quad (1) $$

where α, θ are the rotating angles of yaw channel about k-axis and pitch channel about e-axis respectively; ${}_{P}^{B}T$, ${}_{B}^{A}T$ are the transformation from frame P to B and from frame B to A respectively.

The inertial velocity angular vectors of frame P, B, A respectively are

$$ {}^{P}\overline{\omega_{P/I}} = \begin{bmatrix} \omega_{Pi} \\ \omega_{Pj} \\ \omega_{Pk} \end{bmatrix}, \ {}^{B}\overline{\omega_{B/I}} = \begin{bmatrix} \omega_{Bn} \\ \omega_{Be} \\ \omega_{Bk} \end{bmatrix}, \ {}^{A}\overline{\omega_{A/I}} = \begin{bmatrix} \omega_{Ar} \\ \omega_{Ae} \\ \omega_{Ad} \end{bmatrix}, \quad (2) $$

ω_{pi}, ω_{pj}, ω_{pk} are the body angular velocities of frame P in relation to inertial space about i,j,k axes respectively. ω_{Bn}, ω_{Be}, ω_{Bk} are the body angular velocities of frame B in relation to inertial space n,e,k axes respectively. ω_{Ar}, ω_{Ae}, ω_{Ad} are the body angular velocities of frame A in relation to inertial space r, d, e axes respectively. Inertial matrices of Pitch and Yaw channel respectively are

$$ {}^{A}J = \begin{bmatrix} A_r & A_{re} & A_{rd} \\ A_{re} & A_e & A_{de} \\ A_{rd} & A_{de} & A_d \end{bmatrix}, \ {}^{B}J = \begin{bmatrix} B_n & B_{ne} & B_{nk} \\ B_{ne} & B_e & B_{ke} \\ B_{nk} & B_{ke} & B_k \end{bmatrix}, \quad (3) $$

where A_r, A_e, A_d are moments of inertia about r, e and d axes; A_{re}, A_{rd}, A_{de} are moments products of inertia. B_n, B_e, B_k are moments of inertia about n, e, and k axes; B_{ne}, B_{nk}, B_{ke} are moments products of inertia. Furthermore, in Figure 2, T_p is total external torque about the pitch e-axis, and T_y is total external torque about the pitch k-axis. Based on [2], Euler angles defines the position between two related reference frames. For the base body fixed frame P and the yaw channel fixed frame B with one angle α, these relations can be obtained

$$ \omega_{Bn} = \omega_{Pi}\cos\alpha + \omega_{Pj}\sin\alpha, \ \omega_{Be} = -\omega_{Pi}\sin\alpha + \omega_{Pj}\cos\alpha, \ \omega_{Bk} = \omega_{Pk} + \alpha. \quad (4) $$

Similarly, for the yaw channel fixed frame B and the pitch channel fixed frame A with angle θ, these relations are

$$ \omega_{Ar} = \omega_{Bn}\cos\theta - \omega_{Bk}\sin\theta, \ \omega_{Ad} = \omega_{Bn}\sin\theta + \omega_{Bk}\cos\theta, \ \omega_{Ae} = \omega_{Be} + \dot{\theta}. \quad (5) $$

By applied Newtons second law to rotational motion of two channels of the gimbal system, the external torques applied to the gimbal are [8]

$$ T = \frac{d}{dt}\bar{H} + \bar{\omega} \times \bar{H}, \ \bar{H} = J.\bar{\omega}. \quad (6) $$

$\bar{H} = J.\bar{\omega}$ is the angular momentum, J is the inertia matrix, $\bar{\omega}$ is the angular velocity of the gimbal.

For the yaw channel:

The equation of rotational motion for the yaw channel is

$$T = \frac{d}{dt}\bar{H}_B + \bar{\omega}_{B/I} \times \bar{H}_B. \tag{7}$$

$\bar{H}_B = J_B\bar{\omega}_{B/I} + {}^A_BC^T J_A\bar{\omega}_{A/I}$ is the angular momentum of total gimbal system (expressed in frame B) [4]. The rotation of the yaw channel occurs around the k axis. There for, the motion equation for this channel is the k-component of the equation (7)

$$J_{eq}\dot{\omega}_{BK} = T_y + T_{Dy1} + T_{Dy2}. \tag{8}$$

From (4)

$$J_{eq}\ddot{\alpha} = T_y + T_{Dy1} + T_{Dy2} - J_{eq}\dot{\omega}_{Pk}, \tag{9}$$

where J_{eq} is the instantaneous moment of inertia about k-axis, T_{Dy1}, T_{Dy2} respectively are the disturbances affected the yaw channels rotation cause of the angular motion of the base body and the pitch channels motion (cross-coupling).

$$J_{eq} = B_k + A_r\sin^2\theta + A_d\cos^2\theta - A_{rd}\sin(2\theta), \tag{10}$$

$$\begin{aligned} T_{Dy1} = &\begin{bmatrix} B_n + A_r\sin^2\theta + A_d\sin^2\theta \\ +A_{rd}\sin(2\theta) - (B_e + A_e) \end{bmatrix} \times \omega_{Bn}\omega_{Be} \\ &- \begin{bmatrix} B_{nk} + (A_d - A_r)\sin\theta\cos\theta \\ +A_{rd}\cos(2\theta) \end{bmatrix} (\dot{\omega}_{Bn} - \omega_{Be}\omega_{Bk}) \\ &- (B_{ke} + A_{de}\cos(2\theta) - A_{re}\sin\theta) \times (\dot{\omega}_{Bn} + \omega_{Be}\omega_{Bk}) \\ &- (B_{ne} + A_{re}\cos\theta + A_{de}\sin\theta) \times (\omega_{Bn}^2 - \omega_{Be}^2) + (A_{de}\cos\theta - A_{re}\sin\theta) \times \dot{\omega}_{Bk} \\ &- (A_{de}\sin\theta + A_{re}cos\theta)\omega_{Bk}^2 + \left[B_k + A_r\sin^2\theta + A_d cos^2\theta + A_{rd}\sin(2\theta)\right] \times \dot{\theta}\omega_{Bn} \\ &+ [(A_r - A_d)\sin(2\theta) - 2A_{rd}\cos(2\theta)] \times \omega_{Be}\omega_{Bk}, \end{aligned} \tag{11}$$

$$\begin{aligned} T_{Dy2} =&(A_{re}\sin\theta - A_{de}\cos\theta)\dot{\omega}_{Ae} + (A_{re}\cos\theta + A_{de}\sin\theta){\omega^2}_{Ae} \\ &+ [(A_d - A_r\sin(2\theta) + 2A_{rd}cos(2\theta)] \times \omega_{Ae}\omega_B. \end{aligned} \tag{12}$$

For the pitch channel:

The equation of motion for the pitch channel is

$$T = \frac{d\bar{H}_A}{dt} + \bar{\omega}_{A/I} \times \bar{H}_A, \tag{13}$$

$\bar{H}_A = J_A\bar{\omega}_{A/I}$ is angular momentum for the pitch channel. The rotation of the pitch gimbal occurs about e-axis. Thus, the motion equation obtained from (13) is

$$A_e\dot{\omega}_{Ae} = T_p + T_{Dp1} + T_{Dp2}. \tag{14}$$

From (5)

$$A_e\ddot{\theta} = T_P + T_{Dp1} + T_{Dp2} - A_e\dot{\omega}_{Be}, \tag{15}$$

$$T_{Dp1} = -(A_{de}\sin\theta + A_{re}co\,s\,\theta) \times (\dot{\omega}_{Bn} + \omega_{Be}\omega_{Bk}) + (A_{de}\cos\theta - A_{re}\sin\theta) \times \omega_{Bn}\omega_{Be} + [(A_d - A_r)\cos(2\theta) - 2A_{rd}\sin(2\theta)] \times \omega_{Bn}\omega_{Bk} + \frac{1}{2}[(A_d - A_r)\sin(2\theta) + 2A_{rd}\cos(2\theta)] \times \omega_{Bn}^2, \tag{16}$$

$$T_{Dp2} = (A_{re}\sin\theta - co\,s\,\theta) \times \dot{\omega}_{Bk} - \frac{1}{2}[(A_d - A_r)\sin(2\theta) + 2A_{rd}\cos(2\theta)] \times \omega_{Bk}^2. \tag{17}$$

(9) and (15) can be expressed in the form of state equation and output equation show as

$$\begin{cases} \begin{Bmatrix} \dot{x}_1 \\ \dot{x}_2 \\ \dot{x}_3 \\ \dot{x}_4 \end{Bmatrix} = \begin{Bmatrix} x_3 \\ x_4 \\ \dfrac{1}{A_1}B_1u_1 - C_1x_3x_4 - (D_1 + F_1)x_3 - G_1x_4^2 \\ \dfrac{1}{A_2}B_2u_1 - C_2x_3x_4 - (D_2 + F_2)x_4 - G_2x_3^2 \end{Bmatrix} \\ \begin{Bmatrix} y_1 \\ y_2 \end{Bmatrix} = \begin{Bmatrix} x_1 \\ x_2 \end{Bmatrix}, \end{cases} \tag{18}$$

where $X = [x_1, x_2, x_3, x_4]^T = \left[\theta_1, \alpha_2, \dot{\theta}_1, \dot{\alpha}_2\right]^T$ is state vector, $U = [u_1, u_2]^T$ is the input vector, $Y = [y_1, y_2]^T$ is output vector. $A_1, C_1, D_1, G_1, A_2, C_2, D_2, G_2$ are functions of $\theta_1, \alpha_2, \dot{\theta}_1, \dot{\alpha}_2$ and B_1, F_1, B_2, F_2 are constants.

3. DESIGN THE ADAPTIVE BACKSTEPPING SLIDING MODE CONTROLLER FOR THE TRACKING LOOP

3.1. The backstepping sliding mode controller

The controller design on the basis of backstepping method concludes two steps as follow [18]

Step1. Define

$$X_1 = \begin{bmatrix} x_1 \\ x_2 \end{bmatrix},\ X_2 = \begin{bmatrix} x_3 \\ x_4 \end{bmatrix}$$

as the state vectors of system

$$Y_d = \begin{Bmatrix} y_{1d} \\ y_{2d} \end{Bmatrix}$$

as the reference input of system

$$E_1 = \begin{Bmatrix} e_{11} \\ e_{21} \end{Bmatrix} = \begin{Bmatrix} x_1 - y_{1d} \\ x_2 - y_{2d} \end{Bmatrix},\ E_2 = \begin{Bmatrix} e_{12} \\ e_{22} \end{Bmatrix} = \begin{Bmatrix} x_3 - \dot{y}_{1d} \\ x_4 - \dot{y}_{2d} \end{Bmatrix}$$

as the tracking error.

Define the Lyapunov function in the form of

$$V_1 = \frac{1}{2}{E_1}^T E_1.$$

And the derivative of V_1 can be expressed as

$$\dot{V}_1 = e_{11}e_{12} + e_{21}e_{22},$$

which can not satisfy $\dot{V}_1 < 0$.

Step2. Define the second Lyapunov in the form of

$$V_2 = V_1 + \frac{1}{2}S^T S,$$

where S is the sliding surface vector

$$S = \begin{Bmatrix} s_1 \\ s_2 \end{Bmatrix} = \lambda E_1 + E_2 = \begin{bmatrix} \lambda_1 \\ \lambda_2 \end{bmatrix} \begin{bmatrix} e_{11} \\ e_{21} \end{bmatrix} + \begin{bmatrix} e_{12} \\ e_{22} \end{bmatrix},$$
$$\dot{E}_2 = \begin{bmatrix} \dot{x}_3 \\ \dot{x}_4 \end{bmatrix} = \begin{bmatrix} A_{m1} f(x_i) + B_{m1} u_1 \\ A_{m2} f(x_i) + B_{m2} u_2 \end{bmatrix},$$
$$\lambda_1,\ \lambda_2 > 0.$$

Supposed $\begin{cases} \dot{s}_1 = -\sigma_1 \mathrm{sgn}(s_1) - \beta_1 \\ \dot{s}_2 = -\sigma_2 \mathrm{sgn}(s_2) - \beta_2, \end{cases}$ $\sigma_1,\ \sigma_2,\ \beta_1, \beta_2 > 0.$

Thus, the controller is expressed as

$$\begin{cases} u_1 = \dfrac{1}{B_{m1}} \left(\lambda_1 x_3 + A_{m1} f(x_i) - \sigma_1 \mathrm{sgn}(s_1) - \beta_1 \right) \\ u_2 = \dfrac{1}{B_{m2}} \left(\lambda_2 x_4 + A_{m2} f(x_i) - \sigma_2 \mathrm{sgn}(s_2) - \beta_2 \right), \end{cases} \tag{19}$$

$\beta_1, \beta_2, \lambda_1, \lambda_2$ are chosen for $\beta_1\lambda_1, \beta_2\lambda_2 > \dfrac{1}{2}$ then $\dot{V}_2 \leq 0$.

3.2. The adaptive backstepping controller based on fuzzy logic

The electro-optical system tracks target very accurately under stable environment. However, when working under vibration condition, the system is affected by many disturbances that include dynamic unbalance and cross-coupling effect. The tracking task of system is not accurate and the response is slower. $\beta_1,\ \beta_2$ are the parameters that can affect to the quality of the controller (19). Especially, the task of choosing two parameters is very difficult when the system has to work under vibration environment. Additionally, the control signal contains the sgn() function which makes the chattering phenomenon. The flexible $\beta_1,\ \beta_2$ is the key to reduce the chattering issue. In this paper, the fuzzy logic is proposed to choose two parameters optimally.

The parameters $\beta_1,\ \beta_2$ are tuned by a fuzzy tuner based on the fuzzy model of Takegi-Sugeno-Kang that have s and $\dot{s}$ are inputs. When s and $\dot{s}$ are big, β has to be big to force s to 0 and when s and are small, β has to be small to decrease the chattering. The membership function for input and output are chosen based on the various experiments which authors made in simulation.

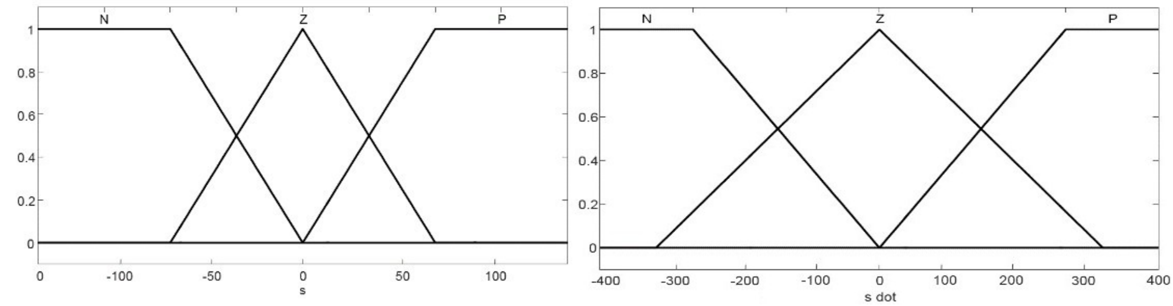

Figure 3. The $s - \dot{s}$ membership function for both channels on Matlab

Table 1. Output value of β_1

	S	M	B
Value	60	140	180

Table 2. Output value of β_2

	S	M	B
Value	2000	3000	4000

Table 3. The fuzzy rule

		s		
		N	Z	P
$\dot{s}$	N	B	M	B
	Z	B	S	B
	P	B	M	B

4. SIMULATION RESULT

In this paper, the working of the Electro-Optical system with the proposed controller will be simulated with different base rates 0, 5, 15 (rad/s) during working under vibration environment. The result of the proposed controller will be compared with the PID controller and the backstepping sliding mode controller to illustrate the efficiency of this controller.

Table 4. The value of inertial moment of the pitch and yaw channel

Parameter	Value ($kg.m^2$)	Parameter	Value ($kg.m^2$)
A_r	0.001	B_n	0.003
A_e	0.0008	B_e	0.0004
A_d	0.006	B_k	0.0003
A_{re}	-0.002	B_{ne}	-0.002
A_{de}	-0.001	B_{ke}	-0.001
A_{rd}	-0.004	B_{nk}	-0.004

- The parameter used in simulation for the backstepping sliding mode controller

$$\beta_1 = 60,\ \beta_2 = 800,\ \lambda_1 = \lambda_2 = 186,\ \sigma_1 = \sigma_2 = 23.$$

- The parameter used in simulation for the conventional PID controller:

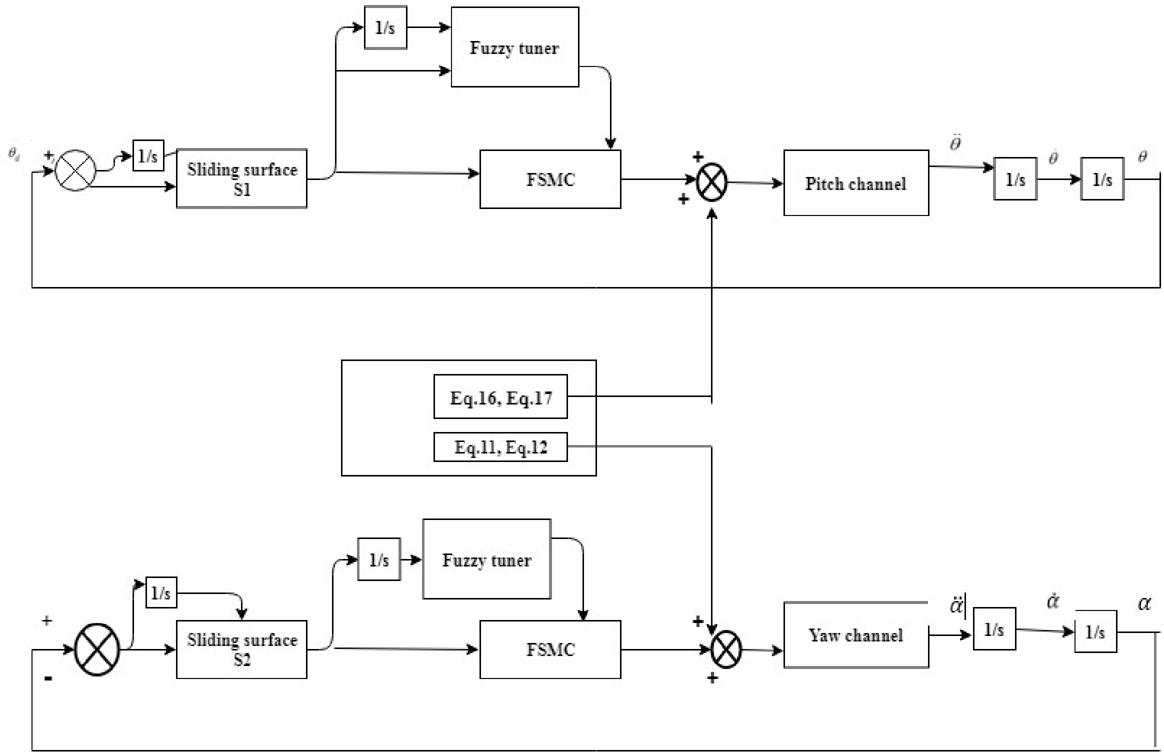

Figure 4. The proposed control architecture

For the pitch channel: $K_p = 65,\ K_I = 4.8,\ K_D = 5$.
For the yaw channel: $K_P = 28,\ K_I = 6,\ K_D = 6$.

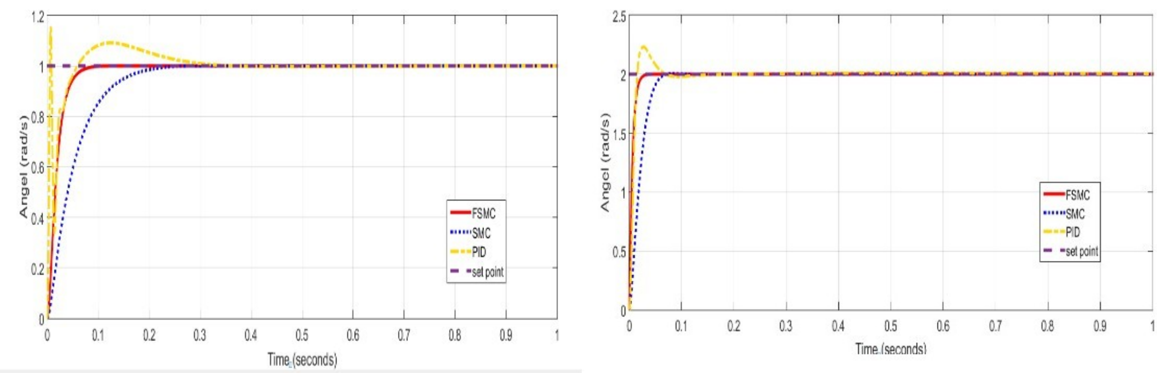

Figure 5. The response of angle of Pitch channel (a) and Yaw channel (b) with $\omega_{Pi} = \omega_{Pj} = \omega_{Pk} = 0$ (rad/s)

Table 5 indicates the adaptive backstepping sliding mode based on fuzzy logic controller is extremely more effective than the PID and the backstepping sliding mode controller, especially when working under vibration environment. If the strength of the PID controller is the fast response time (0,01-0,05s) and the strength of the back stepping sliding mode controller is very small overshoot and steady-state error (0), the proposed controller has both of them. If the overshoot of the system is high, especially when working with the base

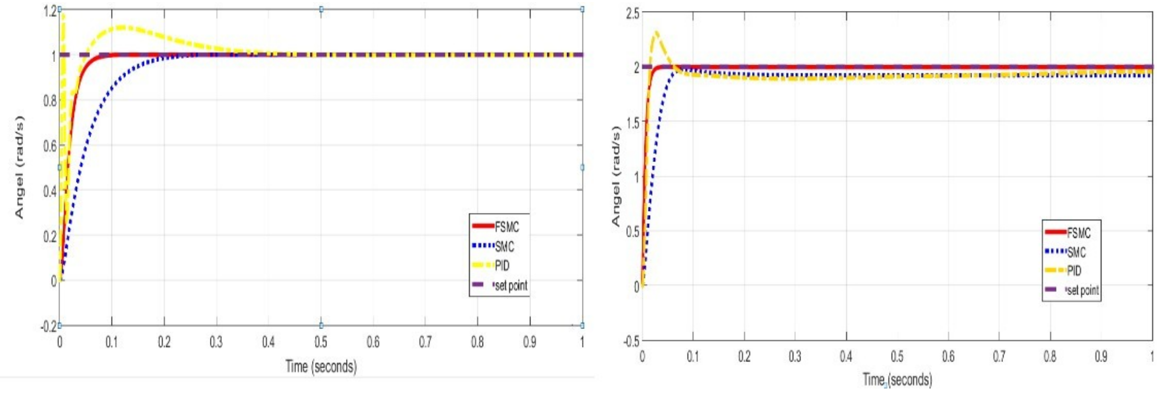

Figure 6. The response of angle of Pitch channel (a) and Yaw channel (b) with $\omega_{Pi} = \omega_{Pj} = \omega_{Pk} = 5$ (rad/s)

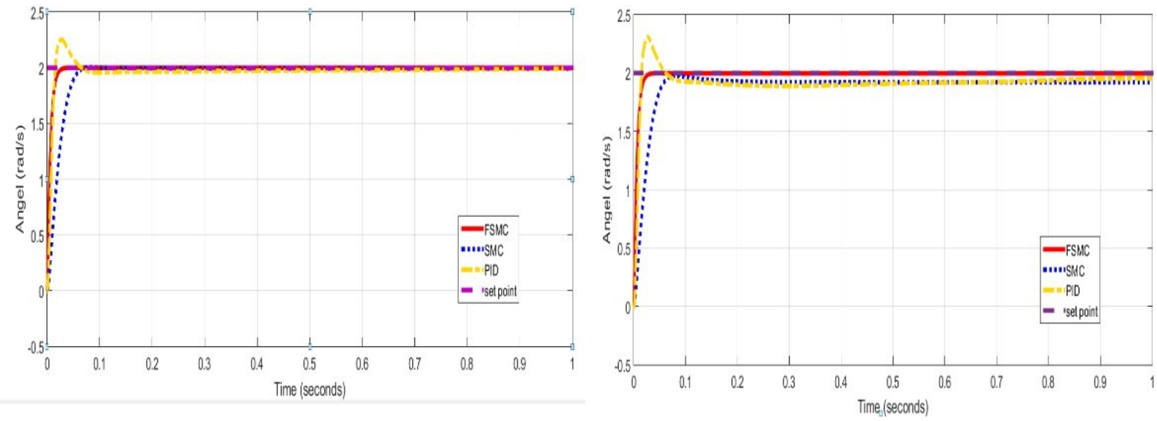

Figure 7. The response of angle of Pitch channel (a) and Yaw channel (b) with $\omega_{Pi} = \omega_{Pj} = \omega_{Pk} = 15$ (rad/s)

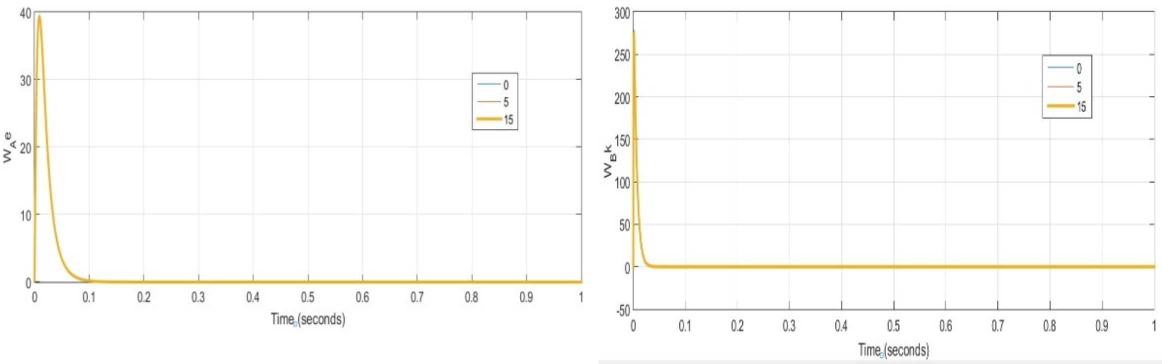

Figure 8. The response of ω_{Bk}(a) and ω_{Ae} (b) with different base rates of FSMC controller

rate 15 rad/s (17,039 for the yaw channel) with the PID controller and the response time of the system with the backstepping sliding mode controller is slower than the PID controller, then the adaptive backstepping sliding mode based on fuzzy logic controller can solve both of them.

Table 5. The simulation results

		Response time (s)			Overshoot (%)			Settling time (s)			Steady-state error (%)		
Base rate (rad/s)	Channel	PID	SMC	FSMC	PID	SMC	FSMC	PID	SMC	FSMC	PID	SMC	FSMC
0	pitch	0.03	0.11	0.03	15.698	0	0	0.352	0.38	0.33	0	0	0
	yaw	0.041	0.05	0.041	13.068	0	0	0.274	0.05	0.044	15	0	0
5	pitch	0.05	0.13	0.05	18.452	0	0	0.3	0.17	0.052	0	0	0
	yaw	0.03	0.05	0.02	13.068	0	0	0.023	0.052	0.021	15	0	0
15	pitch	0.05	0.05	0.13	21.341	0	0	0.605	0.2	0.052	5	0	0
	yaw	0.01	0.06	0.01	17.039	0.314	0	0.1	0.1	0.01	15	5	0

Moreover, the adaptive backstepping sliding mode based on fuzzy logic controller guarantees the rates of the pitch and yaw channel stabilize at 0 rad/s.

5. CONCLUSION

In this paper, an adaptive fuzzy sliding mode controller is proposed for the tracking loop of the electro-optical tracking system when the system works under uncertain environment such as ship, tank or airplane, etc that increases the disturbances on the pitch and the yaw channel. The proposed controller not only guarantees the accuracy of tracking loop, but also solves the weakness of the conventional PID and the back stepping sliding mode controller. The simulation results open the ability to use proposed method in reality when the EOT system has to work on ship, airplane, etc.

REFERENCES

[1] M. Abdo, A. Toloei, A. Vali, and M. Arvan, "Modeling, control and simulation of cascade control servo system for one axis gimbal mechanism," *International Journal of Engineering-Transactions A: Basics*, vol. 27, no. 1, pp. 157–170, 2013.

[2] M. Abdo, A. Toloei, A. R. Vali, and M. R. Arvan, "Cascade control system for two axes gimbal system with mass unbalance," *International Journal of Scientific & Engineering Research*, vol. 4, no. 9, pp. 903–912, 2013.

[3] M. Abdo, A. R. Vali, A. R. Toloei, and M. R. Arvan, "Modeling control and simulation of two axes gimbal seeker using fuzzy pid controller," in *2014 22nd Iranian Conference on Electrical Engineering (ICEE).* Tehran, Iran, May 20–22, 2014, pp. 1342–1347. [Online]. Available: Doi:10.1109/IranianCEE.2014.6999742

[4] M. Abdo, A. R. Vali, A. Toloei, and M. R. Arvan, "Research on the cross-coupling of a two axes gimbal system with dynamic unbalance," *International Journal of Advanced Robotic Systems*, vol. 10, no. 10, p. 357, 2013.

[5] B. Chauhan, M. Singh, V. Sharma, and P. Pandey, "Auto-video tracking system: Performance evaluation," *Defence Science Journal*, vol. 58, no. 4, pp. 565–572, 2008.

[6] E. DiBenedetto, *Classical mechanics: theory and mathematical modeling.* Springer Science & Business Media, 2010.

[7] G. Downey and L. Stockum, “Electro-optical tracking systems considerations,” in *Proceedings Volume 1111, Acquisition, Tracking, and Pointing III.* Orlando, FL, United States, 1989, pp. 70–85. [Online]. Available: https://doi.org/10.1117/12.977971

[8] G. A. Downey, “Electro-optical tracking considerations II,” in *Proceedings Volume 5082, Acquisition, Tracking, and Pointing XVII.* Orlando, Florida, United States, August 04, 2003, pp. 139–154. [Online]. Available: https://doi.org/10.1117/12.487943

[9] M. C. Dudzik, J. S. Accetta, and D. L. Shumaker, “The infrared & electro-optical systems handbook,” *Electro-Optical Systems Design, Analysis, and Testing*, vol. 4, pp. 91–93, 1993.

[10] B. Ekstrand, “Equations of motion for a two-axes gimbal system,” *IEEE Transactions on Aerospace and Electronic Systems*, vol. 37, no. 3, pp. 1083–1091, 2001.

[11] J. Hilkert, “Inertially stabilized platform technology concepts and principles,” *IEEE Control Systems Magazine*, vol. 28, no. 1, pp. 26–46, 2008.

[12] G. C. Holst, *Electro-Optical Imaging System Performance.* JCD Pub., 1995.

[13] H.-P. Lee and I.-E. Yoo, “Robust control design for a two-axis gimbaled stabilization system,” in *2008 IEEE Aerospace Conference.* Big Sky, MT, USA, March 1–8, 2008, pp. 1–7. [Online]. Available: Doi:10.1109/AERO.2008.4526568

[14] R. Nasburg, “Tracking and control systems,” *Electro-Optical Systems Design, Analysis, and Testing*, vol. 4, pp. 263–267, 1994.

[15] N. M. Tien, P. X. Minh, N. D. Nhan, H. T. K. Duyen, and T. T. B. Lien, “Tracking control for the electro optical tracking system based on the self–tuning fuzzy pid control,” *PROCEEDING of Publishing House for Science and Technology*, vol. 1, no. 1, 2016.

[16] B. T. Tuyen and P. T. Cat, “Neural network based visual control,” in *7th International Conference on Control, Automation, Robotics and Vision, 2002. ICARCV 2002.*, vol. 1. IEEE, 2002, pp. 39–44.

[17] Z. Zhao and X. Yuan, “Backstepping designed sliding mode control for a two-axis tracking system,” in *2010 5th IEEE Conference on Industrial Electronics and Applications.* IEEE, 2010, pp. 1593–1598.

[18] ——, “Backstepping designed sliding mode control for a two-axis tracking system,” in *2010 5th IEEE Conference on Industrial Electronics and Applications.* Taichung, Taiwan, June 15–17, 2010, pp. 1593–1598. [Online]. Available: Doi:10.1109/ICIEA.2010.5514728

Received on August 05, 2018
Revised on April 22, 2019